

Supporting Information

Dihydroisocoumarins and dihydroisoflavones from the rhizomes of *Dioscorea collettii* with cytotoxic activity and structural revision of 2, 2'- oxybis (1, 4-di-tert-butylbenzene)

Songsong Jing ^{1,2,†}, Zhuo Qu ^{3,†}, Chengcheng Zhao ², Xia Li ², Long Guo ¹,
Zhao Liu ¹, Yuguang Zheng ^{1,4,*} and Wenyuan Gao ^{2,*}

¹ Traditional Chinese Medicine Processing Technology Innovation Center of Hebei Province, Hebei University of Chinese Medicine, Shijiazhuang 050200, China; johnson3917@163.com (S. J.); guo_long11@163.com (L.G.); liuzhao_mbb@126.com (Z. L.)

² Tianjin Key Laboratory for Modern Drug Delivery & High-Efficiency, School of Pharmaceutical Science and Technology, Tianjin University, Tianjin 300072, China; zhaochengcheng0122@163.com (C. Z.); lix-ia2008@tju.edu.cn (X. L.)

³ School of Pharmacy, Ningxia Medical University, Yinchuan 750004, China; quzhuo2008@163.com (Z. Q.)

⁴ Hebei Chemical & Pharmaceutical College, Shijiazhuang 050200, China

* Correspondence: pharmgao@tju.edu.cn (W.G.); zyg314@163.com (Y.Z.); Tel.: +86-022-87401895 (W.G.)

† These authors contributed equally to this work.

Contents

Figure S1: ^1H -NMR (600 MHz, CD_3OD) spectrum of compound **1a/1b**.

Figure S2: ^{13}C -NMR (150 MHz, CD_3OD) spectrum of compound **1a/1b**.

Figure S3: HSQC spectrum of compound **1a/1b**.

Figure S4: ^1H - ^1H COSY spectrum of compound **1a/1b**.

Figure S5: HMBC spectrum of compound **1a/1b**.

Figure S6: HR-ESI-MS spectrum of compound **1a/1b**.

Figure S7: UV spectrum of compound **1a/1b**.

Figure S8 Chiral HPLC separation chromatogram of compound **1**.

Figure S9: ^1H -NMR (600 MHz, CDCl_3) spectrum of compound **2**.

Figure S10: ^{13}C -NMR (150 MHz, CDCl_3) spectrum of compound **2**.

Figure S11: HSQC spectrum of compound **2**.

Figure S12: ^1H - ^1H COSY spectrum of compound **2**.

Figure S13: HMBC spectrum of compound **2**.

Figure S14 (I). The enlarged HMBC spectrum of compound **2** (I).

Figure S14 (II). The enlarged HMBC spectrum of compound **2** (II).

Figure S14 (III). The enlarged HMBC spectrum of compound **2** (III).

Figure S14 (IV). The enlarged HMBC spectrum of compound **2** (IV).

Figure S15. Structures and comparison of chemical shifts between compounds **2**, **2'** and **2,4-DTBP** in CDCl₃.

Figure S16. ¹H-NMR (600 MHz, C₅D₅N) spectrum of compound **3a/3b**.

Figure S17. ¹³C-NMR (150 MHz, C₅D₅N) spectrum of compound **3a/3b**.

Figure S18. Chiral HPLC separation chromatogram of compound **3**.

Figure S19. ¹H-NMR (600 MHz, C₅D₅N) spectrum of compound **4**.

Figure S20. ¹³C-NMR (150 MHz, C₅D₅N) spectrum of compound **4**.

Figure S21. ECD spectrum of compound **3**

ECD calculation of compound **3**

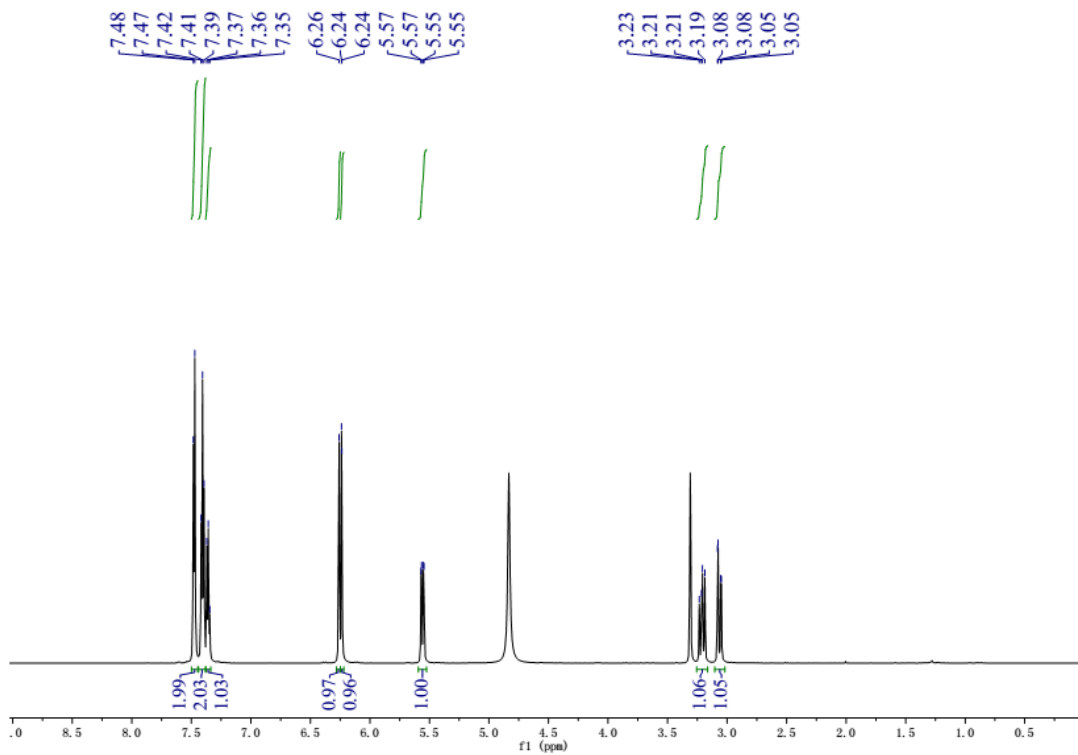


Figure S1. ¹H-NMR (600 MHz, CD₃OD) spectrum of compound **1a/1b**.

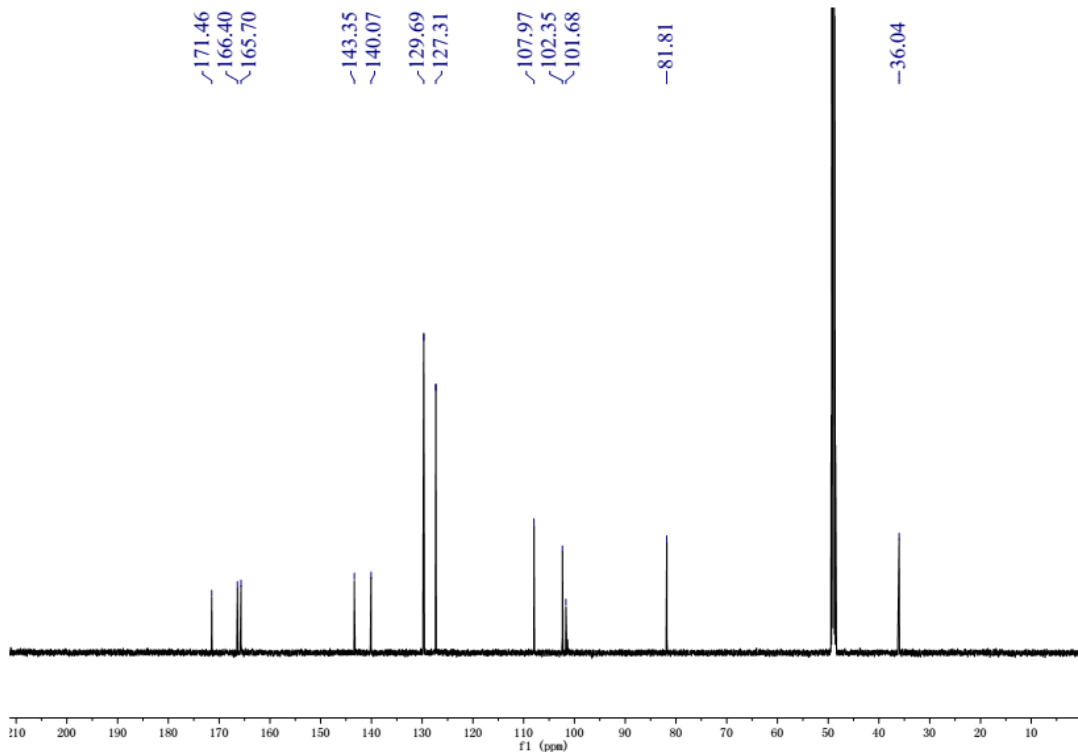


Figure S2. ¹³C-NMR (150 MHz, CD₃OD) spectrum of compound **1a/1b**.

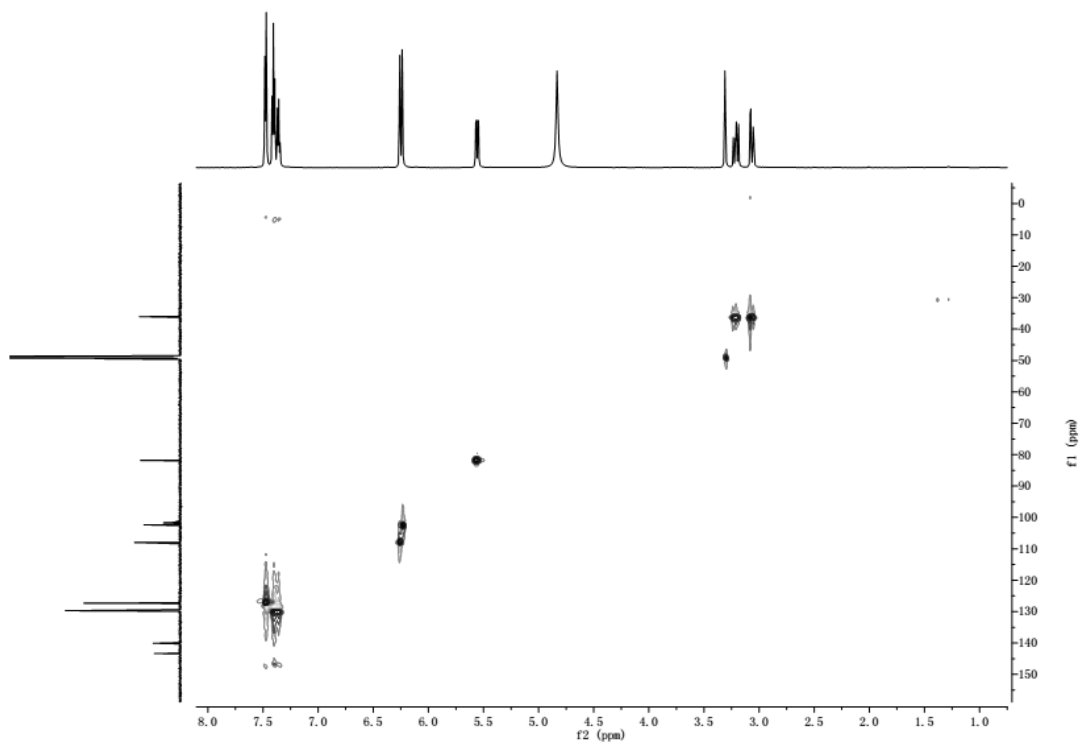


Figure S3. HSQC spectrum of compound 1a/1b.

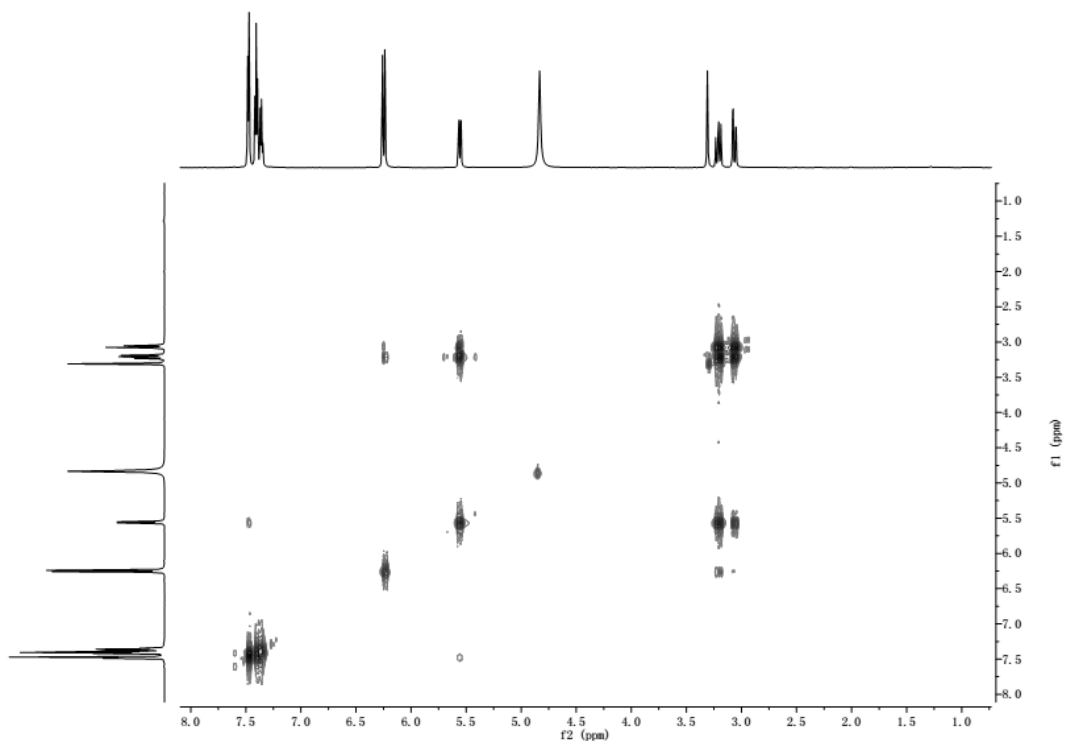


Figure S4. ^1H - ^1H COSY spectrum of compound **1a/1b**.

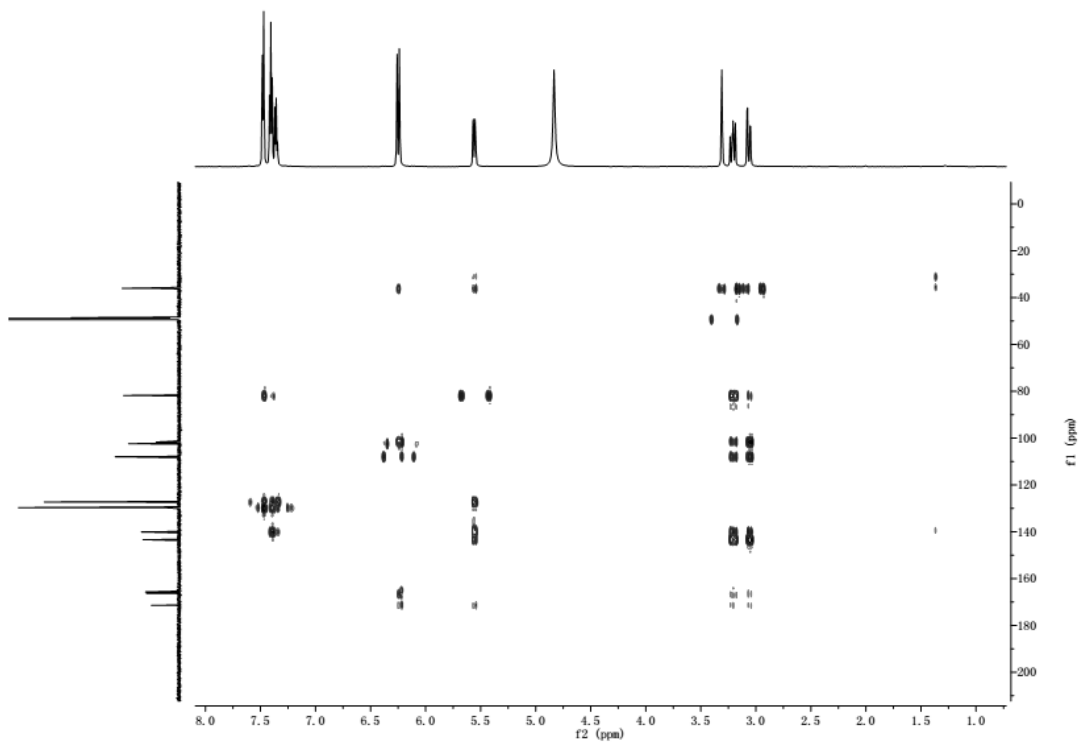
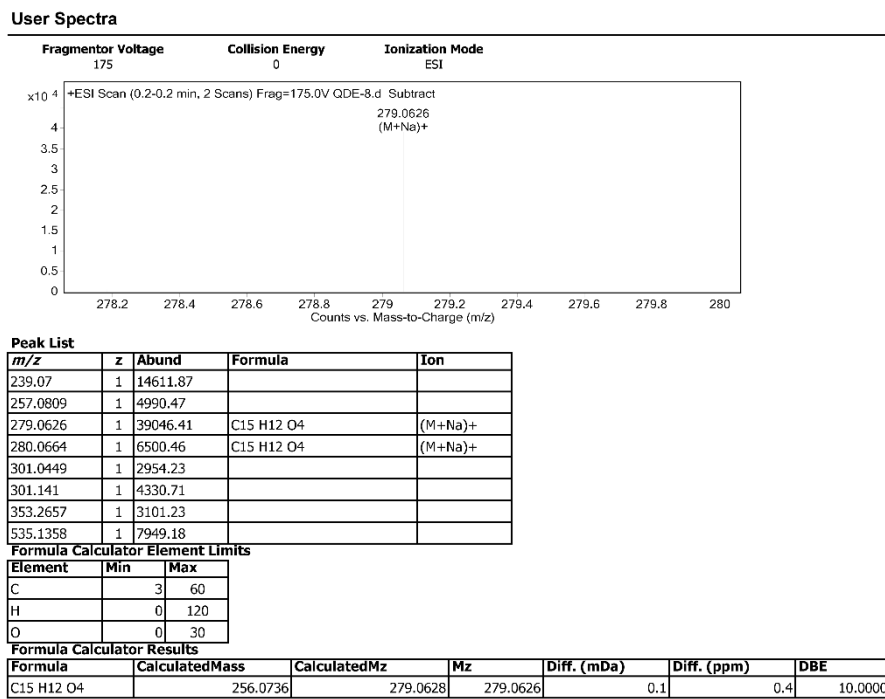


Figure S5. HMBC spectrum of compound **1a/1b**.



--- End Of Report ---

Figure S6. HR-ESI-MS spectrum of compound **1a/1b**.

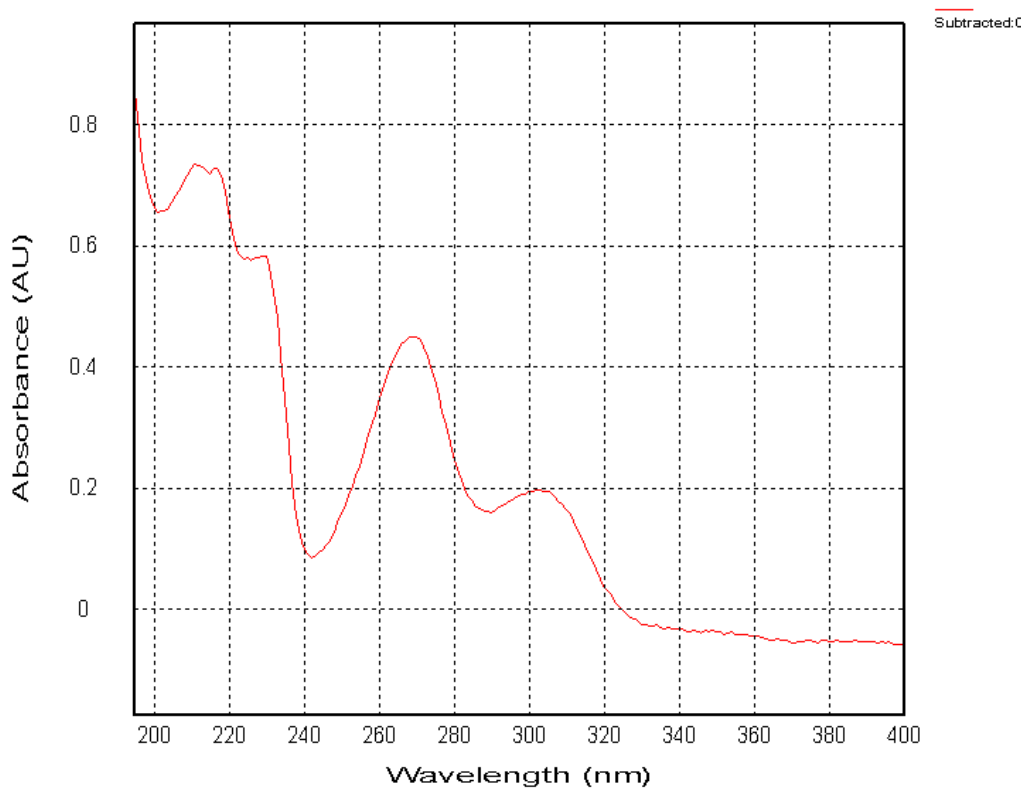


Figure S7. UV spectrum of compound **1a/1b**.

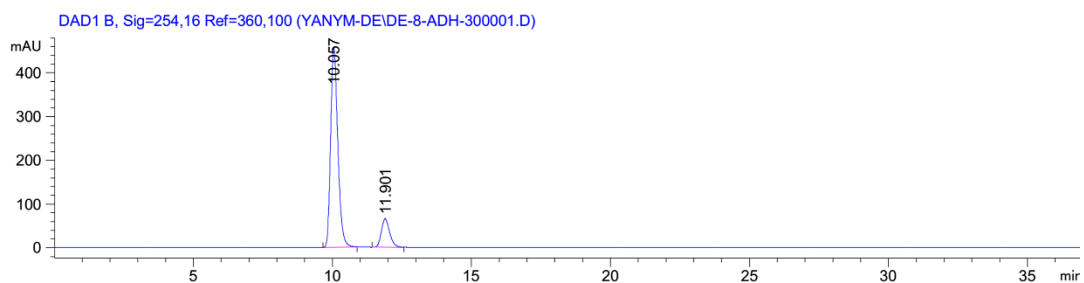


Figure S8. Chiral HPLC separation chromatogram of compound **1**.

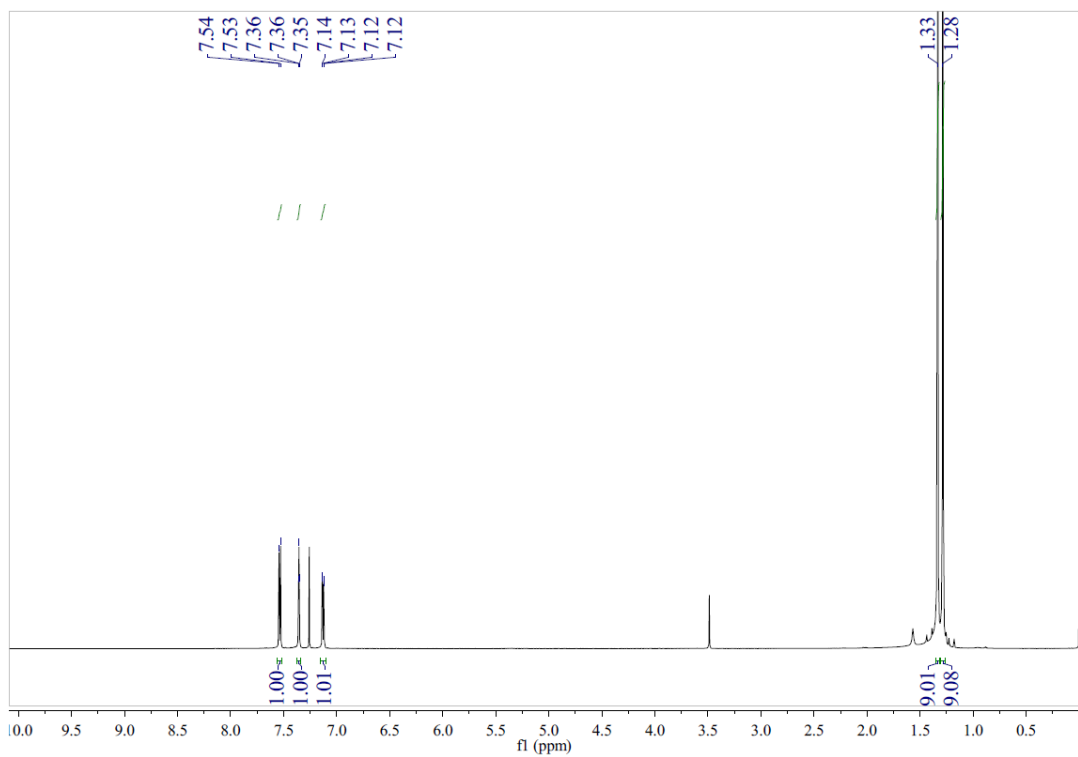


Figure S9. ^1H -NMR (600 MHz, CDCl_3) spectrum of compound 2.

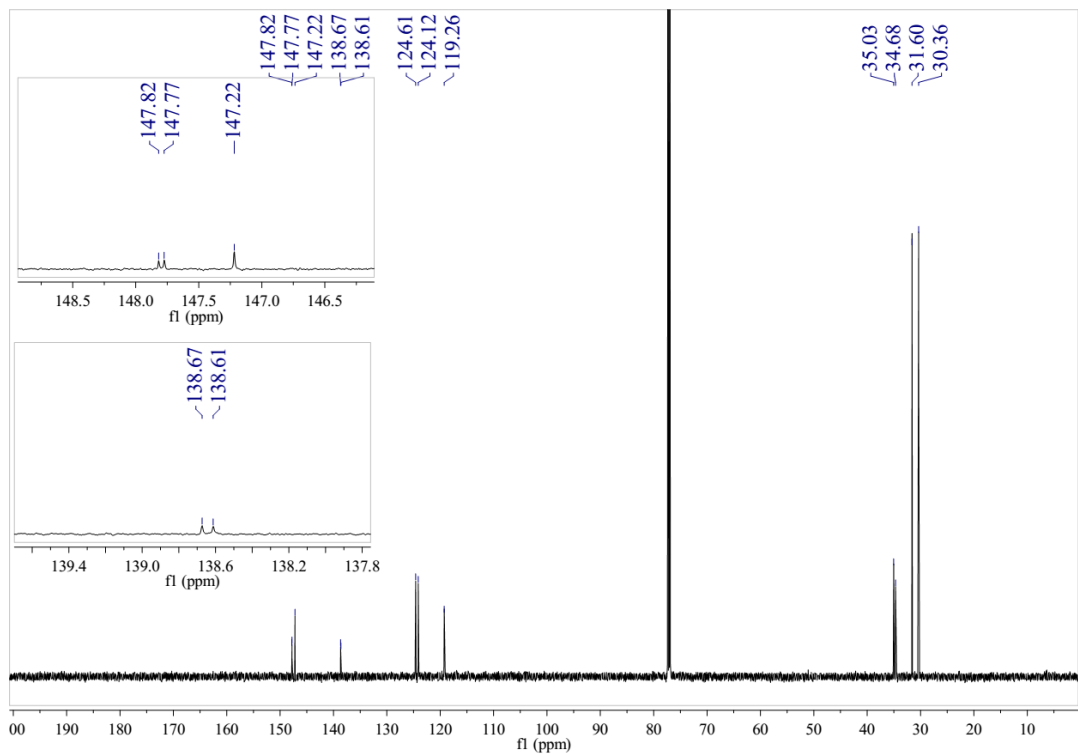


Figure S10. ^{13}C -NMR (150 MHz, CDCl_3) spectrum of compound 2.

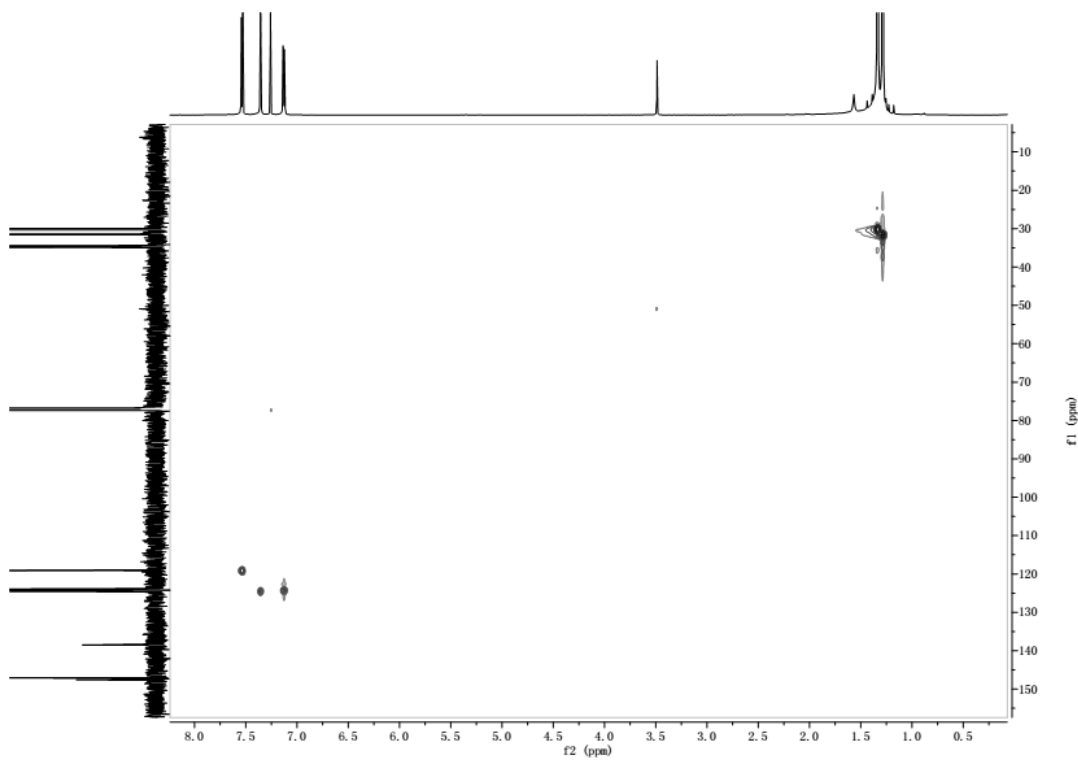


Figure S11. HSQC spectrum of compound **2**.

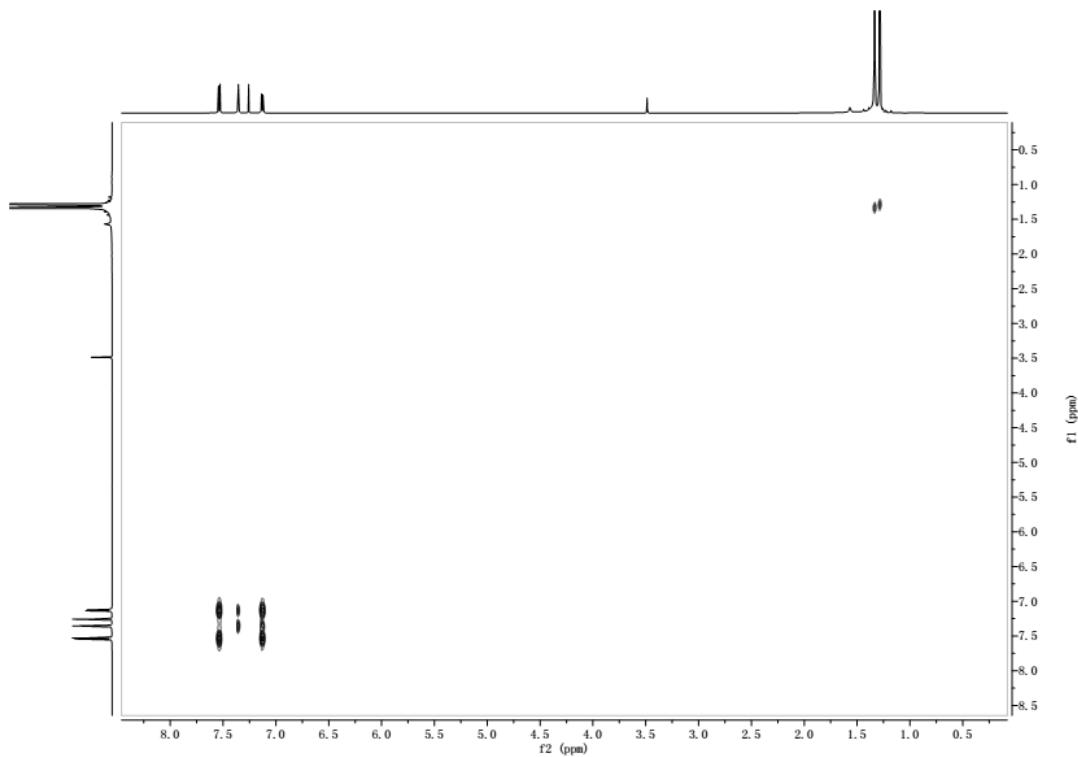


Figure S12. ¹H-¹H COSY spectrum of compound **2**.

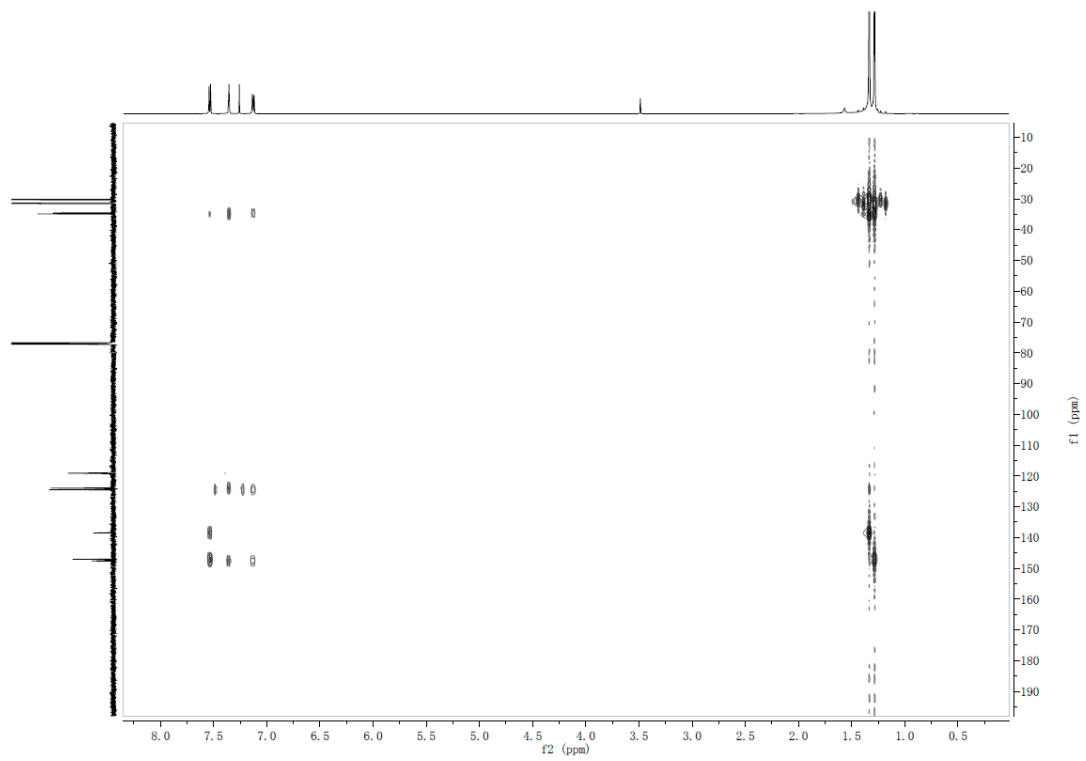


Figure S13. HMBC spectrum of compound 2.

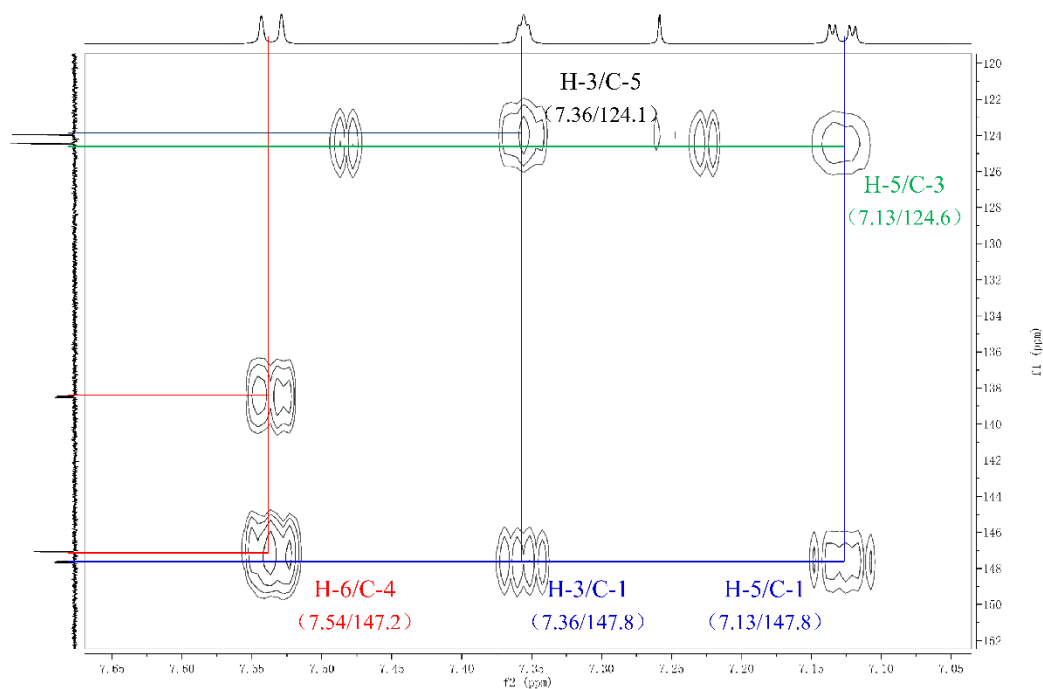


Figure S14 (I). The enlarged HMBC spectrum of compound **2** (I)

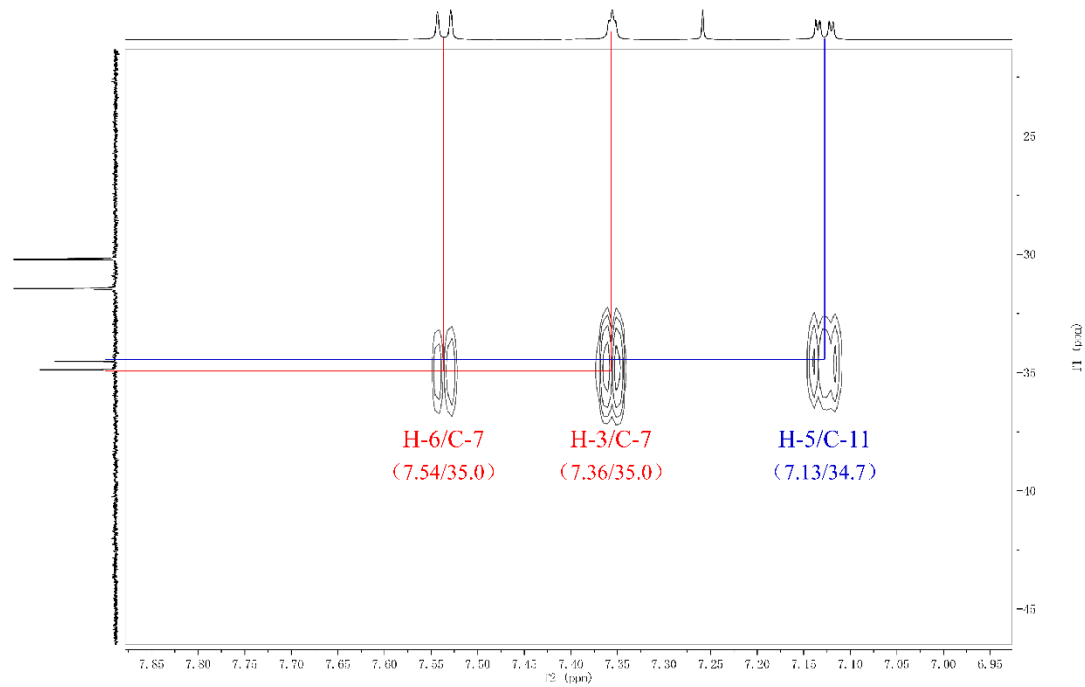


Figure S14 (II). The enlarged HMBC spectrum of compound **2** (II)

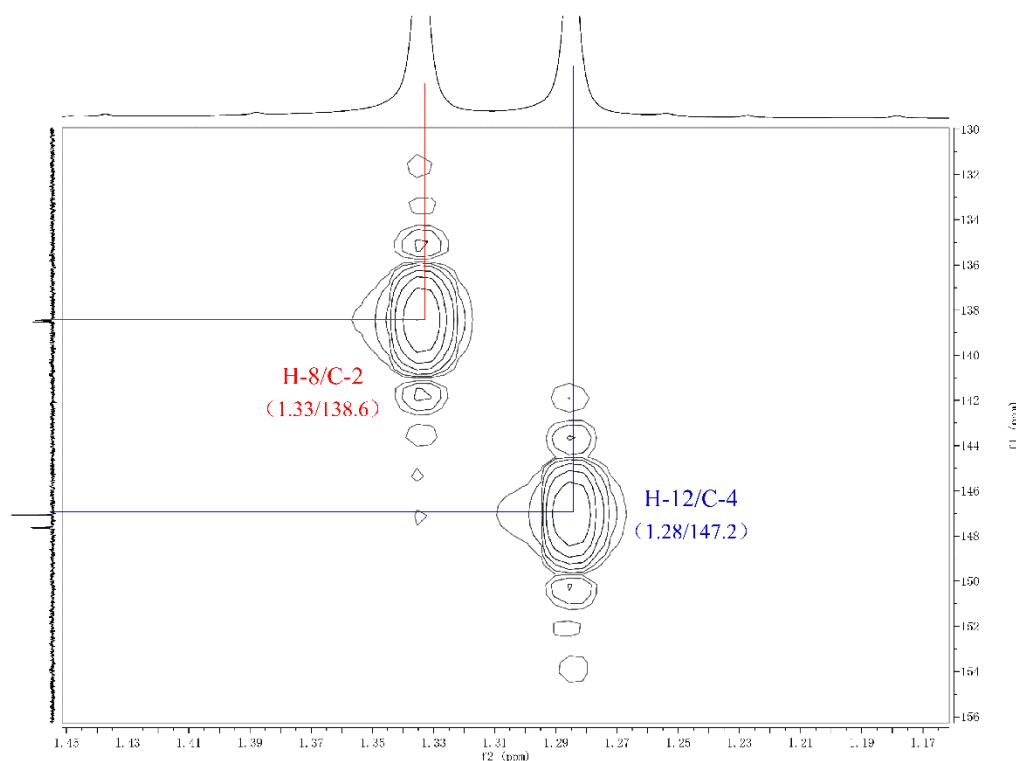


Figure S14 (III). The enlarged HMBC spectrum of compound **2** (III)

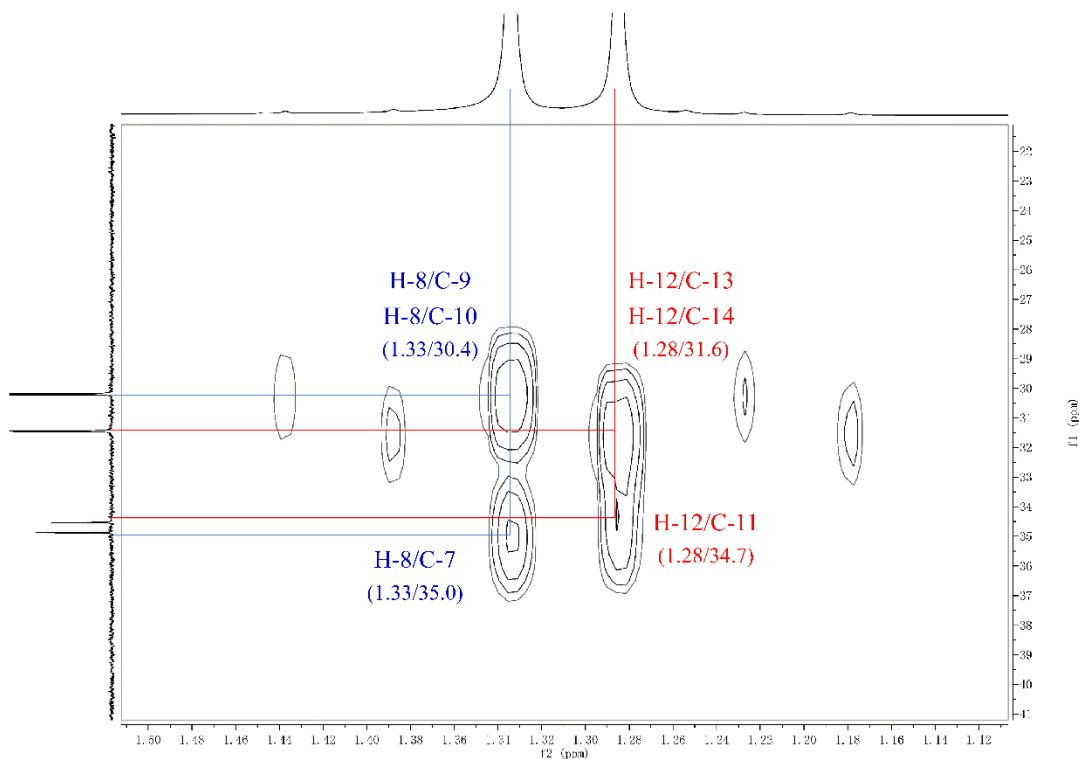


Figure S14 (IV). The enlarged HMBC spectrum of compound **2** (IV)

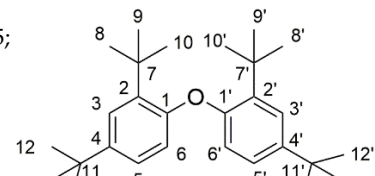
No.	2 ^{a)}		2,4-DTBP ^{b)}		No.	2' ^{c)}	
	δ_H , mult (J in Hz)	δ_C	δ_H , mult (J in Hz)	δ_C		δ_H , mult (J in Hz)	δ_C
1 (1')		147.8 (147.8), C		152.0	2 (2')		147.6 (147.7)
2 (2')		138.6 (138.7), C		135.3	4 (4')		138.5 (138.5)
3 (3')	7.36, t (2.5)	124.6, CH	7.30, br s	124.2	3 (3')	7.36, d (2.5)	124.5
4 (4')		147.2, C		143.1	1 (1')		147.1
5 (5')	7.13, dd (8.6, 2.5)	124.1, CH	7.08, d (8.2)	123.7	5 (5')	7.13, dd (8.7, 2.5)	123.0
6 (6')	7.54, d (8.6)	119.3, CH	6.6, d (8.2)	116.1	6 (6')	7.54, d (8.7)	119.1
7 (7')		35.0, C		34.9	7 (7')		34.9
8/9/10 (8'/9'/10')	1.33, s	30.4, CH ₃	1.42, s	29.8	12/13/14 (12'/13'/14')	1.29, s	30.2
11 (11')		34.7, C		34.4	11 (11')		34.5
12/13/14 (12'/13'/14')	1.28, s	31.6, CH ₃	1.30, s	31.8	8/9/10 (8'/9'/10')	1.33, s	31.4

^{a)} compounds **2**, **2'**, and **2,4-DTBP**, all measured in CDCl₃

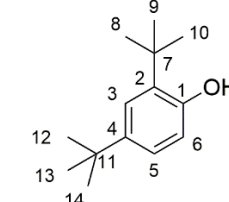
^{b)} **2,4-DTBP**, Journal of Chinese Medicinal Materials, 2019, 07, 1541-1545;

Journal of Ocean University of Qingdao, 1999, 29(1): 53-56.

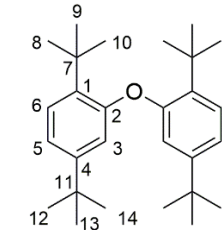
^{c)} **2'**, Natural Product Research And Development, 2014, 26(7): 987-989.



2 revised



2,4-DTBP



2' originally proposed

Figure S15. Structures and comparison of chemical shifts between compounds **2**, **2'**, and **2,4-DTBP** in CDCl₃

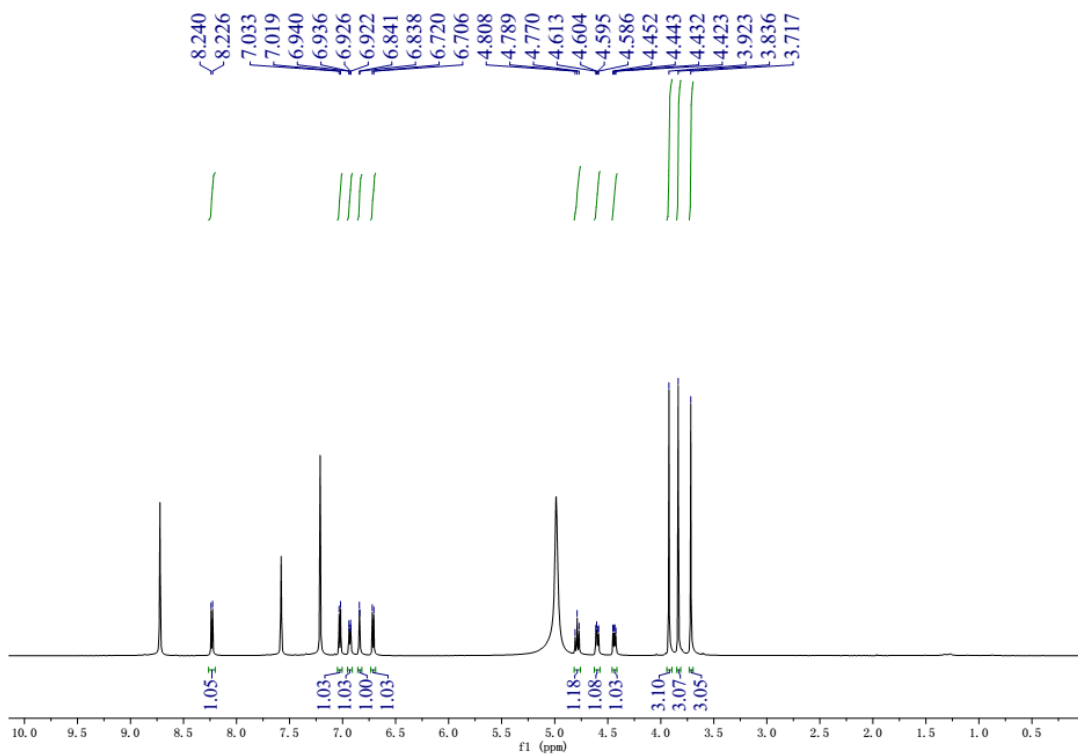


Figure S16. ${}^1\text{H}$ -NMR (600 MHz, $\text{C}_5\text{D}_5\text{N}$) spectrum of compound 3a/3b.

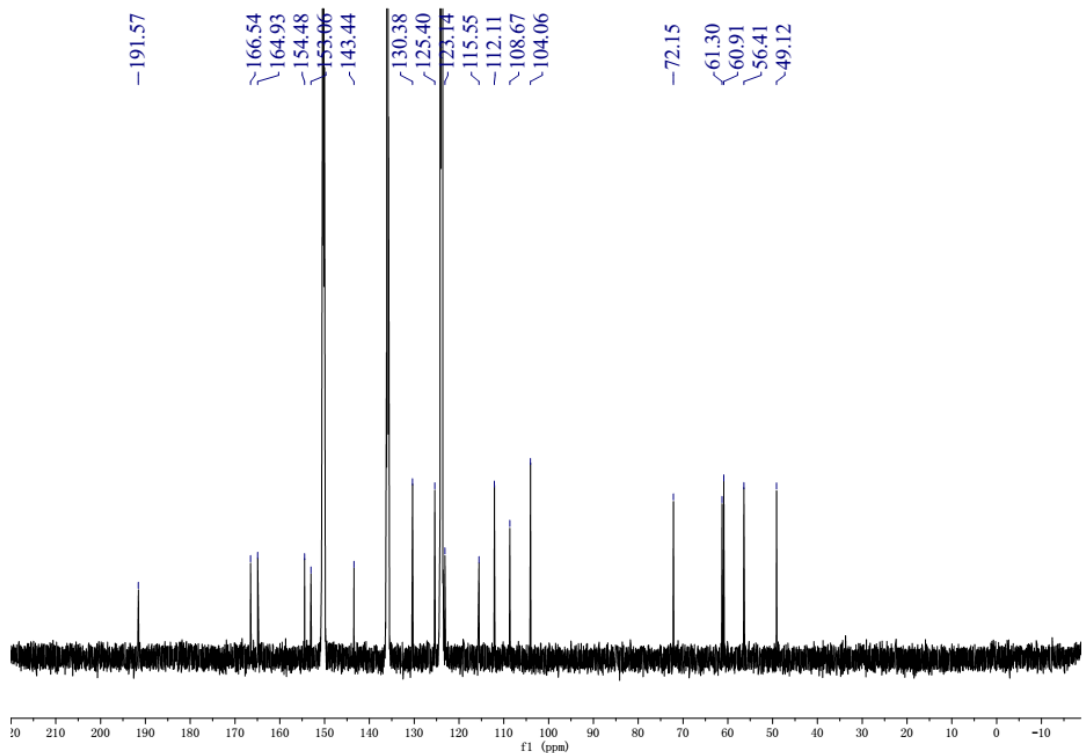


Figure S17. ¹³C-NMR (150 MHz, C₅D₅N) spectrum of compound **3a/3b**.

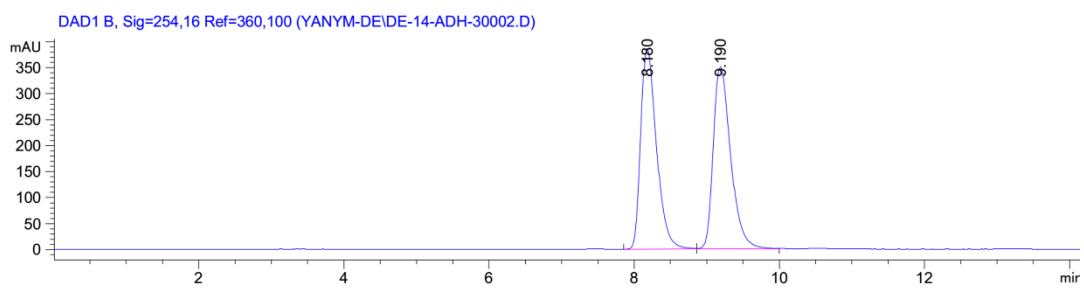


Figure S18. Chiral HPLC separation chromatogram of compound **3**

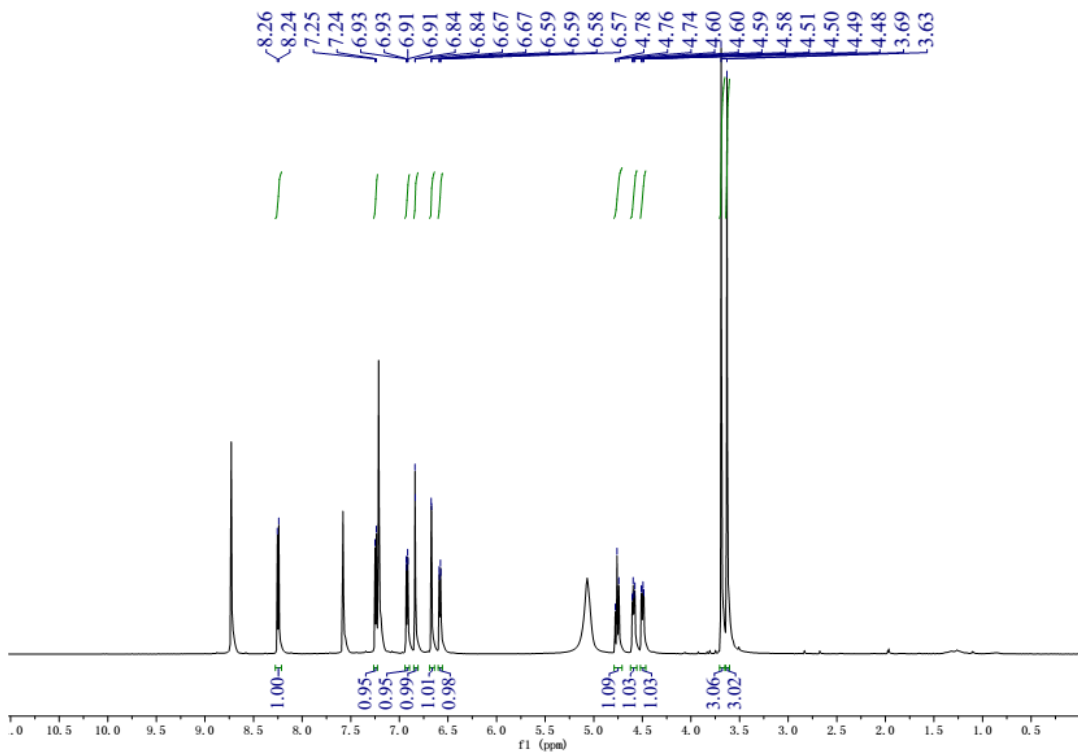


Figure S19. ^1H -NMR (600 MHz, $\text{C}_5\text{D}_5\text{N}$) spectrum of compound 4.

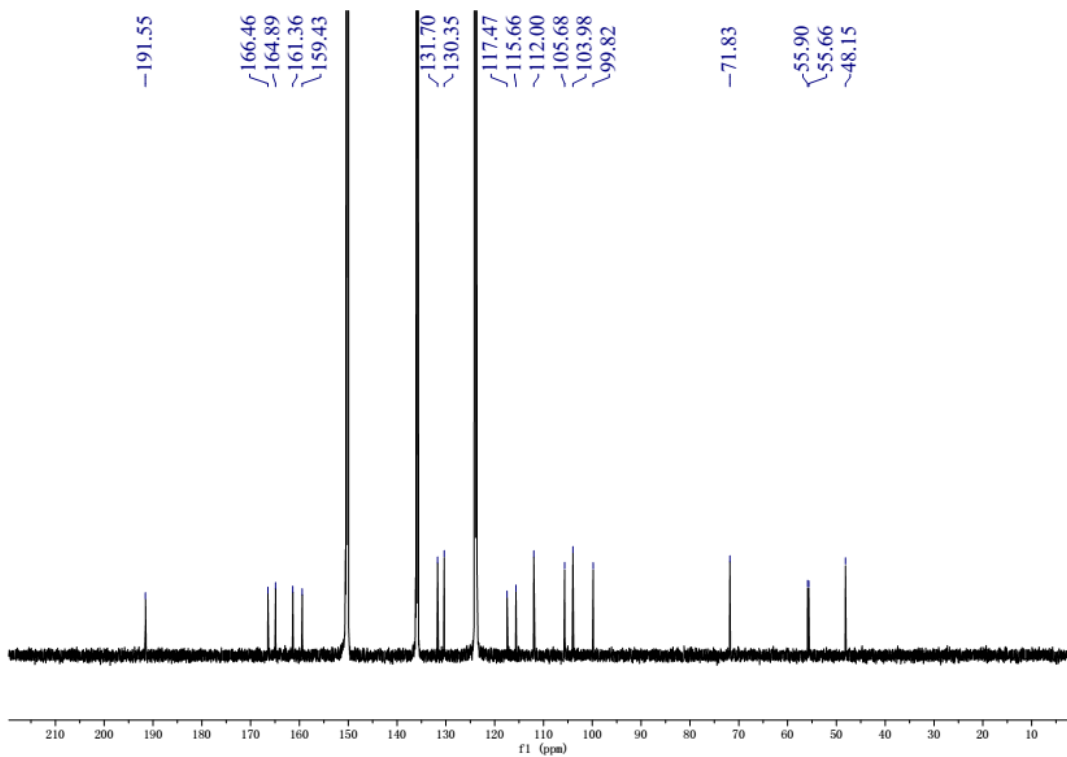


Figure S20. ^{13}C -NMR (150 MHz, $\text{C}_5\text{D}_5\text{N}$) spectrum of compound 4.

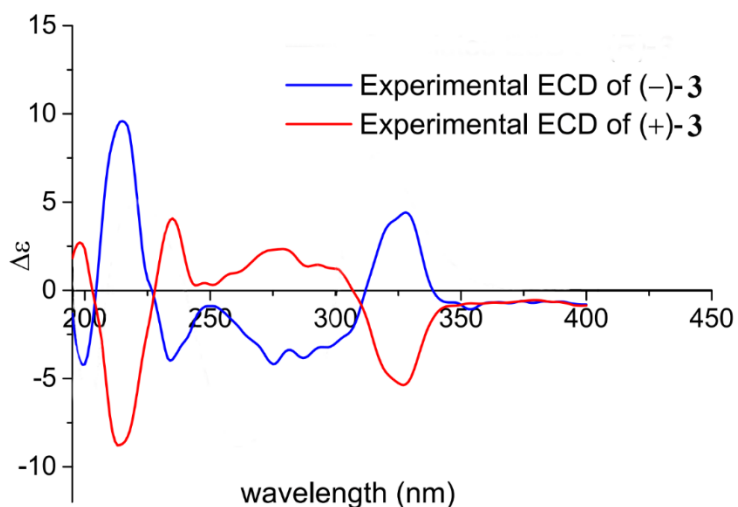


Figure S21. ECD spectrum of compound 3

ECD calculation of compound 3

Computational methods

MMFF94 conformational search generated low-energy conformers within a 10 kcal/mol energy window were performed with CONFLEX.^{1,2} Selected 2 most highest distribution conformers were further optimized by the density functional theory method at the B3LYP/6-31+g(d,p) level. The ECD calculations

was using TD-DFT-B3LYP/6-31+g(d,p) of theory on optimized geometries through the CPCM model (in MeOH). The calculated ECD curves were generated using SpecDis 1.61³ with σ=0.30 ev, UV shift -10 nm. All the above calculations were carried out with the Gaussian 09 package of programs.⁴

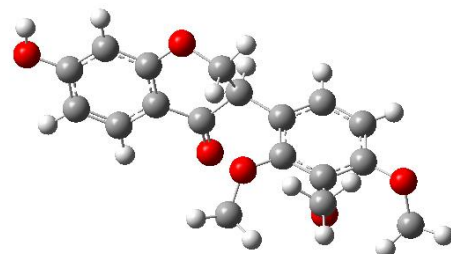
References

- (1) Goto, H.; Osawa, E.; J. Am. Chem. Soc. 1989, 111, 8950–8951.
- (2) Goto, H.; Osawa, E.; J. Chem. Soc., Perkin Trans. 2, 1993, 187–198.
- (3) Bruhn T.; Schaumlöffel A.; Hemberger Y.; Bringmann G.; *SpecDis*, version 1.61, University of Wuerzburg, Germany, 2013.
- (4) Frisch, M. J.; Trucks, G. W.; Schlegel, H. B.; Scuseria, G. E.; Robb, M. A.; Cheeseman, J. R.; Scalmani, G.; Barone, V.; Mennucci, B.; Petersson, G. A.; Nakatsuji, H.; Caricato, M.; Li, X.; Hratchian, H. P.; Izmaylov, A. F.; Bloino, J.; Zheng, G.; Sonnenberg, J. L.; Hada, M.; Ehara, M.; Toyota, K.; Fukuda, R.; Hasegawa, J.; Ishida, M.; Nakajima, T.; Honda, Y.; Kitao, O.; Nakai, H.; Vreven, T.; Montgomery, J. A.; Peralta, J. E.; Ogliaro, F.; Bearpark, M.; Heyd, J. J.; Brothers, E.; Kudin, K. N.; Staroverov, V. N.; Keith, T.; Kobayashi, R.; Normand, J.; Raghavachari, K.; Rendell, A.; Burant, J. C.; Iyengar, S. S.; Tomasi, J.; Cossi, M.; Rega, N.; Millam, J. M.; Klene, M.; Knox, J. E.; Cross, J. B.; Bakken, V.; Adamo, C.; Jaramillo, J.; Gomperts, R.; Stratmann, R. E.; Yazyev, O.; Austin, A. J.; Cammi, R.; Pomelli, C.; Ochterski, J. W.; Martin, R. L.; Morokuma, K.; Zakrzewski, V. G.; Voth, G. A.; Salvador, P.; Dannenberg, J. J.; Dapprich, S.; Daniels, A. D.; Farkas, O.; Foresman, J. B.; Ortiz, J. V.; Cioslowski, J.; Fox, D. J.

Gaussian 09, revision C.01. Gaussian, Inc.: Wallingford CT, 2010.

Coordinates of computations (*R*)-3

Conformer 1

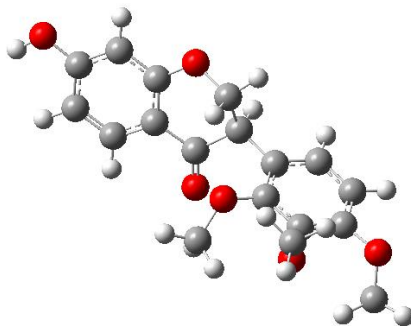


Standard orientation:

Center Number	Atomic Number	Atomic Type	Coordinates (Angstroms)		
			X	Y	Z
1	6	0	5.366836	0.299100	0.070293
2	6	0	4.855214	0.876661	-1.109917
3	6	0	3.520746	0.695089	-1.420807
4	6	0	2.657795	-0.045064	-0.584106
5	6	0	3.193468	-0.597480	0.601542
6	6	0	4.544021	-0.434792	0.925734
7	6	0	1.268833	-0.317238	-0.981097
8	6	0	0.480166	-1.228821	-0.032839
9	6	0	1.017340	-1.100706	1.399586
10	8	0	2.441024	-1.330678	1.463931
11	8	0	0.790300	0.080473	-2.043673
12	8	0	6.686479	0.503823	0.330057
13	6	0	-1.023005	-1.047529	-0.085305
14	6	0	-1.857639	-2.138776	-0.353070
15	6	0	-3.246449	-2.006028	-0.378855
16	6	0	-3.831625	-0.770028	-0.102047
17	6	0	-3.018398	0.338560	0.199558
18	6	0	-1.616816	0.203446	0.173190
19	8	0	-0.797116	1.265467	0.482051
20	6	0	-0.862229	2.416606	-0.389261
21	8	0	-3.607018	1.547371	0.497907

22	6	0	-3.662957	1.852424	1.906003
23	8	0	-5.204015	-0.673971	-0.046807
24	6	0	-5.815548	0.090236	-1.103957
25	1	0	5.516985	1.444925	-1.754197
26	1	0	3.109806	1.114015	-2.333391
27	1	0	4.926502	-0.870228	1.843716
28	1	0	0.707141	-2.249249	-0.375750
29	1	0	0.809776	-0.103628	1.801238
30	1	0	0.574673	-1.854501	2.051172
31	1	0	6.946563	0.070940	1.156668
32	1	0	-1.412285	-3.108054	-0.558006
33	1	0	-3.886840	-2.853761	-0.599551
34	1	0	-0.626820	2.117831	-1.414782
35	1	0	-1.846557	2.886090	-0.343863
36	1	0	-0.100175	3.105234	-0.021757
37	1	0	-4.244432	1.092219	2.438427
38	1	0	-2.655719	1.916338	2.329548
39	1	0	-4.160019	2.820126	1.987324
40	1	0	-6.889535	0.063532	-0.913724
41	1	0	-5.461776	1.124504	-1.092999
42	1	0	-5.603039	-0.370181	-2.075666

Conformer 2



Standard orientation:

Center Number	Atomic Number	Atomic Type	Coordinates (Angstroms)		
			X	Y	Z
1	6	0	5.368445	0.285590	0.087946
2	6	0	4.861560	0.871867	-1.090176
3	6	0	3.525460	0.695417	-1.405319
4	6	0	2.660476	-0.046437	-0.575443
5	6	0	3.193020	-0.606540	0.610156
6	6	0	4.541067	-0.449426	0.937435
7	6	0	1.271253	-0.312654	-0.977599
8	6	0	0.478636	-1.227213	-0.035826
9	6	0	1.012389	-1.106152	1.398638
10	8	0	2.434461	-1.342220	1.465769
11	8	0	0.796446	0.092229	-2.038999
12	8	0	6.672480	0.414409	0.455013
13	6	0	-1.024277	-1.045148	-0.091059
14	6	0	-1.858513	-2.135753	-0.362740
15	6	0	-3.247335	-2.003352	-0.388516
16	6	0	-3.832925	-0.768417	-0.107863
17	6	0	-3.020135	0.339544	0.197127
18	6	0	-1.618486	0.204845	0.171074
19	8	0	-0.799256	1.266069	0.484068
20	6	0	-0.863417	2.419366	-0.384323
21	8	0	-3.609264	1.547262	0.498850
22	6	0	-3.665174	1.848522	1.907756
23	8	0	-5.205353	-0.673097	-0.051952
24	6	0	-5.817691	0.092829	-1.107293
25	1	0	5.516177	1.445864	-1.739437
26	1	0	3.118715	1.120598	-2.316905
27	1	0	4.934463	-0.884195	1.849376
28	1	0	0.705995	-2.246366	-0.382334
29	1	0	0.807037	-0.109768	1.803316
30	1	0	0.564630	-1.860532	2.046069

31	1	0	7.155745	0.950617	-0.190675
32	1	0	-1.412777	-3.104320	-0.570202
33	1	0	-3.887419	-2.850640	-0.611785
34	1	0	-0.102994	3.107867	-0.013210
35	1	0	-0.625211	2.123528	-1.410069
36	1	0	-1.848337	2.887753	-0.340124
37	1	0	-4.246117	1.086544	2.438226
38	1	0	-2.657925	1.911903	2.331345
39	1	0	-4.162825	2.815695	1.991747
40	1	0	-6.891524	0.065833	-0.916249
41	1	0	-5.463862	1.127070	-1.094965
42	1	0	-5.605998	-0.365979	-2.079961